A Boundary Element Method with Reduced-basis for Computing Electrical Field around Long Slim Conductors

Chijie Zhuang[1], *Member, IEEE*, Yong Zhang[2], Rong Zeng[1], *Senior Member, IEEE* and Jinliang he[1], *Fellow, IEEE*

[1]State Key Lab of Power System, Department of Electrical Engineering, Tsinghua University, Beijing 100084, China
[2]Wolfgang Pauli Institute, Nordbergstrasse 15, 1090 Vienna, Austria

Evaluation of surface electric fields, which is well described by Poisson equation, is of great importance in shielding failure evaluation in power system. This paper proposes a boundary element method with reduced surface density basis considering the fact the radius of the transmission line is much smaller than its length. Examples show the method is convergent and is more accurate than charge simulation method which is often used for the evaluation of surface electric field of long slim conductors.

***Index Terms*—surface electric field, boundary element method, charge simulation method.**

I. Introduction

Evaluation of surface electric fields is of great importance in computation of the shielding failure in power system that is modelled by Leader Propagation Method (LPM) [1]. In LPM, the electric field is treated as electrostatic or quasi-electrostatic field, and the electric potential is well described by Poisson equation.

The conductors are assumed in the electrostatic states, the charges shall distribute on the conductor surface, therefore it would be more reasonable to apply some surface density based method, like boundary element method (BEM) [2].

Boundary element method has been widely used in science and engineering. It is efficient when surface/volume ratio is typically small and is suitable for unbounded exterior problem. Considering the fact that the radius of a transmission line is much smaller compared with its length, we propose a boundary element method with reduced surface density basis.

II. Collocation boundary element method

Consider a finite horizontal transmission line shown in Fig. 1 as a right cylinder of length $2L_0$ and radius R_0, we set the axis of the cylinder as x axis and the vertical direction as z axis. Define the unbounded domain $\Omega = \mathbb{R}^3 \setminus \overline{\Omega'}$ where Ω' denotes the cylinder and we use bold letters to denote points throughout the whole paper. Let $\Sigma = \Sigma_{\rm B} \bigcup \Sigma_{\rm L}$ denotes the boundary surface of Ω where $\Sigma_{\rm B}$ the base surface along the conductor and the $\Sigma_{\rm L}$ the two sides of the conductor.

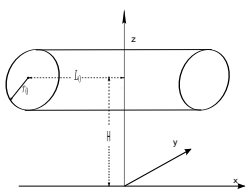

Fig. 1. Exterior Laplace Equation

we choose collocation BEM for its simplicity. The segment $[-L_0, L_0]$ on x-axis is first equally discretized as $x_j = jh_x$, $j = -N_x, \cdots, N_x$ with $h_x = \frac{L_0}{N_x}$ and N_x being a positive integer. The radius is also equally discretized as $r_k = kh_r, k = 0, \ldots, N_r$ with $h_r = \frac{R_0}{N_r}$ and N_r being a positive integer. Then we discretize the surface by cylinder element on lateral surface and by ring element on base surface.

The potential and its normal derivative belongs to function space V, which is defined as

$$V = \{f(\mathbf{x}) :\ f_h(\mathbf{x})\big|_{\Sigma_B}, f_h(\mathbf{x})\big|_{\Sigma_L} \text{ are continuous}\}. \quad (2.1)$$

Because the radius/length ratio, i.e., R_0/L_0, is small, it is reasonable to assume the potential and its normal derivative to be axial symmetric. A reduced space V_h is introduced as follows

$$\begin{aligned} V_h \ = \ & \{f_h(\mathbf{x}) :\ f_h \in V,\ f_h(\mathbf{x})\big|_{e_L^j} = f_h(x) \text{ is linear,} \\ & f_h(\mathbf{x})\big|_{e_{B-}^k} = f_h(r), f_h(\mathbf{x})\big|_{e_{B+}^k} = f_h(r) \text{ are linear,}\} \end{aligned}$$

with $h := \max(h_r, h_x)$.

Notice that for $f \in V$ and $f_h \in V_h$, they are continuous on lateral Σ_L or base surface Σ_B, but they are not necessarily continuous over the whole surface Σ, especially at circles where the lateral and base surface intersects. Generally speaking, the normal derivative is discontinuous at the intersection circles due to discontinuity in normal vector. To treat the discontinuity, we apply discontinuous element [2] for elements that include the intersection circles, i.e., $e_L^{\pm N_x}$, $e_{B\pm}^{N_r}$.

Define an interpolation operator $P : V \to V_h$ as follows:

$$(Pf)(\mathbf{x}_i) = f(\mathbf{x}_i), \quad \forall\, \mathbf{x}_i \in \Lambda, \quad \forall f \in V. \quad (2.2)$$

We omit $\tilde{}$ in (2.2) for sake of simplicity. Then we try to find $u_{\mathbf{n},h} \in V_h$, which is an approximation to $u_{\mathbf{n}}$, such that

$$\begin{aligned} \alpha(\mathbf{x}_i)\,(Pu)(\mathbf{x}_i) + \oint_\Sigma (Pu)(\mathbf{y})\ \partial_{\mathbf{n_y}} G(\mathbf{x}_i, \mathbf{y})\,\mathrm{d}S_{\mathbf{y}} = \\ \oint_\Sigma G(\mathbf{x}_i, \mathbf{y})\ u_{\mathbf{n},h}(\mathbf{y})\,\mathrm{d}S_{\mathbf{y}}, \quad \forall\, \mathbf{x}_i \in \Lambda. \end{aligned}$$

The above equation is written in matrix form as

$$[A, B] \begin{pmatrix} \tau_{2(N_r+1)} \\ \eta_{2N_x+1} \end{pmatrix} = \phi_{N\times 1} \quad (2.3)$$

where $\tau_{2(N_r+1)}$ is a column vector of the surface densities on both undersides and η_{2N_x+1} is a column vector of the lateral surface densities. Matrix $C_{N\times N} = [A, B]$ is the coefficient matrix, with its entries C_{ij} representing potential at x_i generated by the j-th unit vector $(\tau^T_{2(N_r+1)}, \eta^T_{2N_x+1}) = (0, \ldots, 0, 1, 0, \ldots, 0)$. The formation of coefficient matrix involve two kinds of surface integral, i.e., ring element surface integral on underside and cylindrical element integral on lateral surface. Using the symmetry property, the surface integral can be simplified, which can help reduce computation cost. As is common in BEM, singular/nearly-singular surface integral has to be dealt with very carefully, while for regular integral, Guassian quadrature is applicable.

III. Numerical Results

A. Convergene of CBEM

Example 1 Consider a finite cylinder without ground. The cylinder is specified as $R_0 = 0.5, L_0 = 10$. We choose the exact solution $u_{\text{ext}}(\mathbf{x}) = \frac{1}{|\mathbf{x}|}$ as a benchmark. The boundary condition is thus prescribed as $g(\mathbf{x}) = u_{\text{ext}}\big|_{\Sigma}$. To resolve the potential on unbounded domain Ω by CBEM, we just need to solve normal derivative distribution, i.e. $\partial_{\mathbf{n}} u_{\text{ext}}$, on surface.

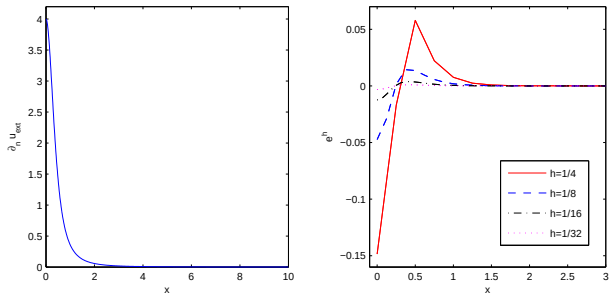

Fig. 2. Convergence results of CBEM in example 1. (left) exact normal derivative distribution on surface; (right) errors e^h with different mesh h.

From Fig. 2, we can see that e^h diminishes uniformly as mesh size h goes to zero. Then the numerical solution $u^h_{\mathbf{n}}$ converges uniformly.

B. Comparison of CBEM and CSM

Apart from CBEM, CSM is a favorable alternative in electromagnetic computation due to its simplicity and efficiency [4], [3], and is suitable for long slim conductors. We can apply CSM and place simulation line charge along the central axis. The line charge density is assumed to be a piecewise linear function along the axial direction. As stated before, although CSM can solve the Laplace equation efficiently, however it may cause some unphysical phenomenon that will be illustrated in Example 2.

Example 2 Consider a finite cylinder without ground. The cylinder is specified with $R_0 = 1.68\times10^{-2}$. Constant Dirichlet boundary condition is set as $g(\mathbf{x}) = 5 \times 10^4$.

Some convergence results of CBEM and CSM are proposed when L_0=10. Fig. 3 shows the normal derivative $u^h_{\mathbf{n}}$ by CBEM versus the x-axis on lateral surface and radial direction on underside surface with different mesh size h. Fig. 4 shows the

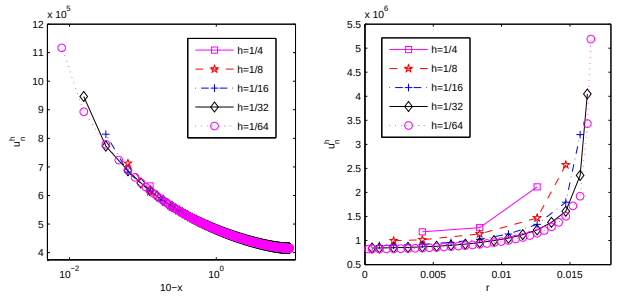

Fig. 3. Normal derivative $u^h_{\mathbf{n}}$ with different mesh h by CBEM in Example 2. (left) $u^h_{\mathbf{n}}$ along the x-axis on lateral surface; (right) $u^h_{\mathbf{n}}$ in r direction on underside surface.

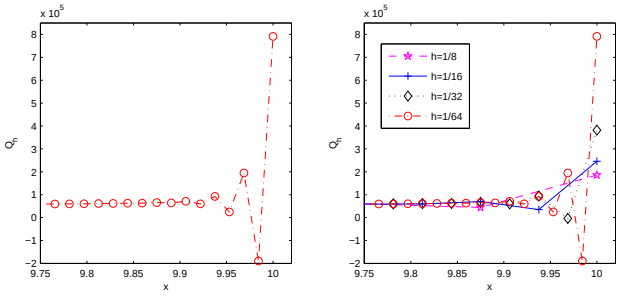

Fig. 4. Line charge density Q_h by CSM in Example 2. (left) Q_h verse x with fine mesh $h = 1/64$; (right) Q_h verse x near right end with different mesh h.

line charge density Q_h by CSM along the right half segment and the variance of Q_h near the right end for $x \in [9.5, 10]$. It can be concluded that surface charge density by CBEM converges uniformly while line charge density by CSM only converges pointwisely. The nonphysical oscillation by CSM in line charge density near cylinder ends may be caused mainly by the disregard of the underside charge.

IV. Conclusions

This paper proposes a boundary element method with reduced surface density basis considering the fact that the radius of a transmission line is much smaller compared with its length. Examples show the method is convergent and is more accurate than charge simulation method which is often used to compute the surface electric field for long slim conductors. More comparisons will be given in the full version manuscript.

References

[1] R. Zeng, Y.N. Geng, Y. Li, J.L. He, Lightning shielding failure model of transmission line based on leader progress model, High Voltage Engineering, 34 (10), 2008.

[2] J.T. Katsikadelis, Boundary Elements: Theory and Applications, Elsevier Science, 2002.

[3] B. Zhang, J.L. He, X. Cui, S.J. Han and J. Zou, Electric field calculation for HV insulators on the head of transmission tower by coupling CSM with BEM, IEEE Transactions on Magnetics, 42(4), 2006.

[4] Z.Z. Li, Z.Y. Wang,R. Zeng, Y. Zhang, Z.Q. Yu, Research on characteristics of conductor surface electric field considering downward lightning leader, 2010 Asia-Pacific Symposium on Electromagnetic Compatibility (APEMC).